Available online at www.sciencedirect.com

ScienceDirect

Procedia Structural Integrity 2 (2016) 1716–1723

Structural Integrity Procedia

www.elsevier.com/locate/procedia

21st European Conference on Fracture, ECF21, 20-24 June 2016, Catania, Italy

# Micromechanical cohesive zone relations for ductile fracture

Tuncay Yalçinkaya[a,*], Alan Cocks[b]

[a] Middle East Technical University, Department of Aerospace Engineering, Ankara 06800, Turkey
[b] University of Oxford, Department of Engineering Science, Parks Road, Oxford OX1 3PJ, UK

**Abstract**

This paper addresses the derivation of a micromechanically motivated incremental mixed-mode traction separation law in the context of cohesive zone modeling of crack propagation in ductile metallic materials. The formulation is based on the growth of an array of pores idealized as cylinders which are considered as the representative volume elements. An upper bound solution is applied for the deformation of the representative volume element and different incremental traction-separation relations are obtained for mixed-mode loading conditions. While most of the current traction-separation relations used in cohesive zone modeling consider phenomenological relations, in the current work micromechanical parameters such as size, shape and spacing of pores describe the level of damage and linkage of the pores characterizes the propagating crack.


Peer-review under responsibility of the Scientific Committee of ECF21.

*Keywords:* ductile fracture; cohesive zone modeling; micromechanics; micro void growth; porous plasticity; limit load analysis

## 1. Introduction

The underlying physical mechanism for the ductile fracture of engineering metallic materials is the generation of considerable porosity (void volume fraction), where micro voids nucleate, grow and coalesce. Typically the initial porosity is found to be in the range of $10^{-4}$ to $10^{-2}$ (see e.g. Tvergaard (1990), Thomason (1990)). The experimental studies illustrates that the voids start to coalesce and eventually ductile failure occurs when the void volume fraction reaches values from 0.1 to 0.3 (see e.g. Barbee et al. (1972), Beachem and Yoder (1973), Cortes (1992)). In ductile materials, the voids nucleate at inclusions and second–phase particles, by decohesion of the particle-matrix interface or by particle cracking. Therefore, void growth is driven by plastic deformation of the surrounding matrix. This phenomenon has been subjected to extensive research and implemented in (porous) plasticity and creep models over the last 40 years (see e.g. McClintock (1968), Gurson (1977), Cocks and Ashby (1980), Tvergaard and Needleman (1984), Rousselier (1987), Cocks (1989), Gologanu et al. (1993), Gologanu et al. (1994)) and used for damage initiation predictions. The main idea is that plasticity behavior of the material is governed by both the mean and deviatoric stresses including both material hardening and geometric softening effects.

* Corresponding author. Tel.: +90-312-210-4258 ; fax: +90-312-210-4250.
*E-mail address:* yalcinka@metu.edu.tr


Peer review under responsibility of the Scientific Committee of ECF21.
10.1016/j.prostr.2016.06.217

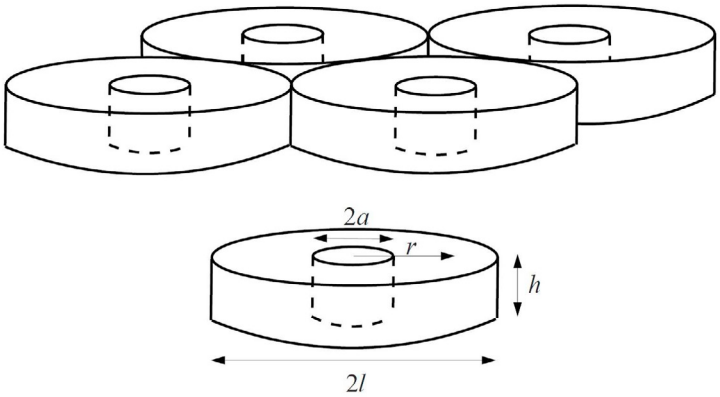


Fig. 1. Idealization of pores within a plane as cylinders.

Considering damage/crack propagation the so-called cohesive zone models, introduced as a plane in front of the crack tip, has been a widely used approach for ductile fracture. Within this approach the fracture process is represented through a traction-separation law for the cohesive zone. This approach was first introduced by Barenblatt (1962) and subsequently used by Tvergaard and Hutchinson (1992) for modeling crack propagation in ductile materials. The material separation is described by interface elements, following the traction-separation law, which is a phenomenological image of the fracture process, lacking the physical insight of the problem. There is no evidence to guide the choice of cohesive law and a number of functions have been proposed in the literature (see e.g. Brocks et al. (2003) for an overview). The maximum traction or so-called cohesive strength, the critical separation value where the traction becomes zero and the area under traction-separation curve which is called cohesive energy are the basic ingredients of such models. The form of the cohesive law is independent of the material but related to the separation mechanism. In this context, the purpose of this paper is to bridge the information obtained from the physical fracture mechanism due to void growth to a traction-separation law to derive a micromechanical relation to be implemented in crack propagation simulations. Classical cohesive zone models of the type described above can be viewed as being equivalent deformation models of plasticity. Here we develop an incremental model for the cohesive zone for mixed mode loading. Following the approach of Cocks Cocks (1989) the response is expressed in terms of scalar potential quantities. We idealize porosity in the cohesive zone as a regular array of cylindrical pores, as employed by McClintock (1968) and Cocks and Ashby (1980). A number of authors (see e.g. Marin and McDowell (1996)) have demonstrated that bulk models based on idealization of this type provide a good description of the behavior of a number of ductile alloys. This gives some confidence in applying the same methodology to identify a suitable structure for the description of cohesive zone behavior for ductile fracture. The paper is organized as follows. First the mode-I traction-separation relation is derived through Minkowski inequality and plotted in terms of volume fraction and geometry of pores. Then, after analyzing the mixed-mode loading case the calculation of work of fracture is addressed and the paper is concluded through some remarks.

## 2. Formulation of the model

In this section the mode-I and the mixed-mode traction-separation relations are derived and the methodology for the calculation of work of fracture is presented. Following the upper bound for a perfectly plastic material the traction separation relations are presented in terms of morphological parameters or through a yield function formulation.

### *2.1. Mode-I loading*

Consider an array of pores within a plane, which are idealized as cylinders (see Fig. 1). Let the radius of the pores at a given instant be $a$, the mean spacing $2l$ and the height of the cylinders be $h$. Isolate a representative cell and

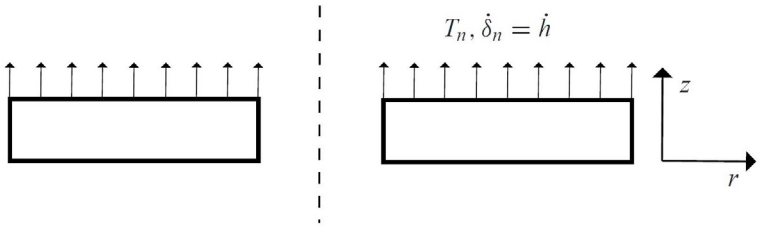


Fig. 2. Loading of the representative cell.

assume that all cells remain the same. Also assume that deformation is concentrated in these zones, i.e. there is an axial macroscopic strain, however the in plane macroscopic strain is zero, i.e. if $u$ is the radial displacement in the plane, $u = 0$ at $r = l$.

Initially we consider the response to transverse traction $T_n$ (see Fig. 2). The initial volume of a pore is $\pi a_0^2 h_0$. The representative cell is fully constrained so that $l$ remains constant. Through the incompressibility condition in the matrix material, $\dot{\varepsilon}_r + \dot{\varepsilon}_\theta + \dot{\varepsilon}_z = 0$ and using the small strain-displacement relations in polar coordinates $\dot{\varepsilon}_z = \dot{h}/h, \dot{\varepsilon}_\theta = \dot{u}/r, \dot{\varepsilon}_r = \dot{u}/dr$ and the boundary conditions ($\dot{u} = 0$ at $r = l$) we get $\dot{u} = (\dot{\varepsilon}_z r/2)/(l^2/r^2 - 1)$ and other strain rate components becomes

$$\dot{\varepsilon}_\theta = \frac{\dot{u}}{r} = \frac{\dot{\varepsilon}_z}{2}(\frac{l^2}{r^2} - 1) \quad \text{and} \quad \dot{\varepsilon}_r = -(\dot{\varepsilon}_\theta + \dot{\varepsilon}_z) = -\frac{\dot{\varepsilon}_z}{2}(\frac{l^2}{r^2} + 1) \tag{1}$$

Next we apply the upper bound for a perfectly plastic material, where work done by the limit load is smaller or equal to the integral of internal energy dissipation of the effective strain rate $\dot{\varepsilon}_e$ at yield stress

$$\pi l^2 T_n \dot{\delta}_n \leq \int_a^l \dot{\varepsilon}_e \sigma_y 2\pi r h dr \tag{2}$$

Using (1) the effective strain rate could be written as

$$\dot{\varepsilon}_e = \dot{\varepsilon}_z \sqrt{1 + \frac{l^4}{3r^4}} \tag{3}$$

Substituting (3) into inequality (2) and using $\dot{\delta}_n = \dot{h}$ and $\dot{\varepsilon}_z = \dot{h}/h$ gives

$$T_n \leq \sigma_y \int_f^1 \sqrt{1 + (1/3v^2)} dv \quad \text{where} \quad v = r^2/l^2 \quad \text{and} \quad dv = 2r/l^2 dr \tag{4}$$

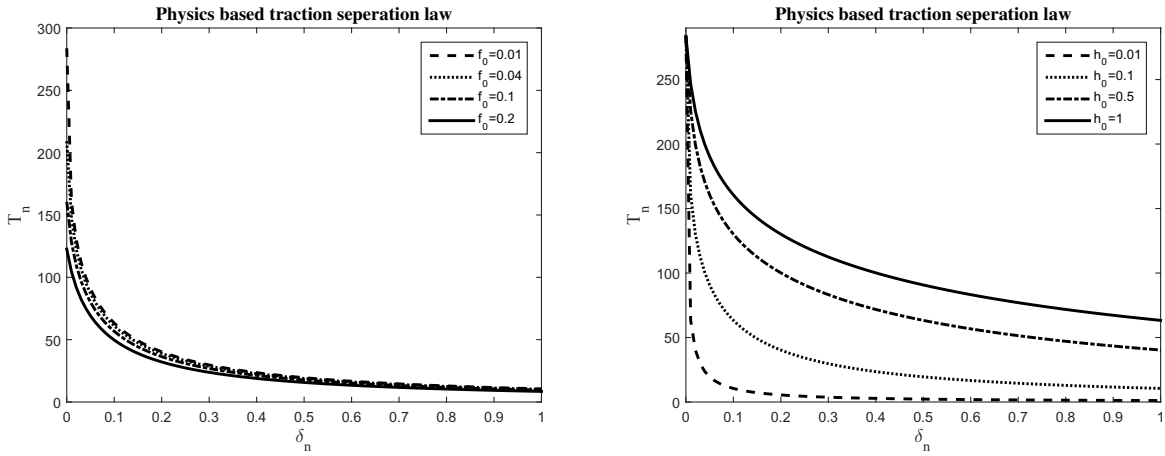


Fig. 3. Dependence of mode-I traction-separation law on initial height of voids and volume fraction with $\sigma_y = 100$MPa and $h_0 = 0.01\mu$m (top) and $f_0 = 0.01$ (bottom) using the Minkowski inequality.

Here $f = a^2/l^2$ is the area fraction of pores in the plane of the cavitated zone. In order to retain analytical expressions for the constitutive response of the cohesive, the integral in (4) can be estimated by using the Minkowski inequality $\left(\int (f+g)^k dx\right)^{\frac{1}{k}} > \left(\int f^k dx\right)^{\frac{1}{k}} + \left(\int g^k dx\right)^{\frac{1}{k}}$ or Jensen's inequality $\int (f+g)^k dx < \int f^k dx + \int g^k dx$ (see e.g. Hardy et al. (1996)). Applying the Minkowski inequality and using (4) gives

$$T_n \approx \sigma_y \left( (1-f)^2 + (\frac{1}{\sqrt{3}} \ln \frac{1}{f})^2 \right)^{\frac{1}{2}} . \tag{5}$$

Applying Jensen's inequality would retain the formal nature of the upper bound calculation (see Yalcinkaya and Cocks (2015)), but the Minkowski inequality generally provides a better estimate of the full integral and results in a continuous single equation for the yield function under multiaxial loading (see section 2.2) rather than the discontinuous function when using Jensen's inequality (see Yalcinkaya and Cocks (2015)). However, here we have indicated that formally the result is an approximation and no longer an upper bound, because the Minkowski inequality is the opposite sense to that of the upper bound. Practically (5) provides a yield function, which can be calibrated by comparison with experimental behavior.

Assume that $f = f_0$ when $h = h_0$ and consider the following relation again: $df/(1-f) = dh/h$ and integration gives $\ln([1-f_0]/[1-f]) = \ln(h/h_0)$ or simply $h = h_0(1-f_0)/(1-f)$, and if $\delta_n = h - h_0$ this gives $\delta_n = h_0(f-f_0)/(1-f)$ and $f = (\delta_n + h_0 f_0)/(\delta_n + h_0)$. Then using (5) we get

$$T_n = \sigma_y \left[ \left( \frac{h_0(1-f_0)}{(\delta_n + h_0)} \right)^2 + \left( \frac{1}{\sqrt{3}} \ln \left( \frac{(\delta_n + h_0)}{(\delta_n + h_0 f_0)} \right) \right)^2 \right]^{\frac{1}{2}} \tag{6}$$

which is an alternative representation of the mode-I traction separation law and its dependence on the initial volume fraction of pores and height of the pore. The mode–I traction–separation relation is illustrated in Fig. (3) for different initial height of voids and volume fraction values and in Fig. (4) traction versus normalized separation/initial height ratio is presented.

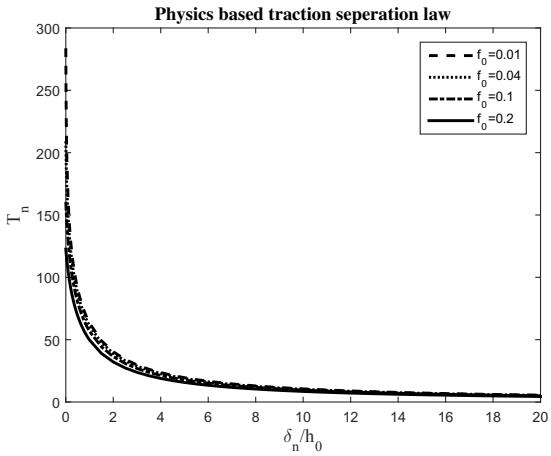


Fig. 4. Traction versus separatoin/initial height ratio for mode-I loading with $\sigma_y = 100$MPa using the Minkowski inequality.

## 2.2. Mixed-mode loading

Now consider combined normal and tangential loading. Note that under shear loading pores become more crack like and elongate in the direction of shear Fleck and Hutchinson (1986). The previous analysis shows that as a result of $\dot{\delta}_n$ pore volume increases and therefore $f$ increases $df = d\delta_n/h(1-f)$.

Under shear loading the shape of the pores change (see Fig. (5a)). We consider a new shape where cylinders have modified radius and height (see Fig. (5b). Considering shear deformation does not change the volume we have $\pi a^2 h = \pi(a + d\delta_t)^2(h - dh) = \pi a^2 h + 2\pi a h d\delta_t - \pi a^2 dh$ resulting in $dh/h = 2(d\delta_t/a)$. Writing $f$ as $f = a^2/l^2$ gives $df = (2a/l)(da/l) = 2\sqrt{f}(d\delta_t/l)$. Then we have the following relations for combined normal and shear deformation.

$$
\begin{aligned}
df &= \frac{d\delta_n}{h}(1-f) + 2\sqrt{f}\frac{d\delta_t}{l} \\
dh &= d\delta_n - 2\frac{h}{a}d\delta_t
\end{aligned}
\tag{7}
$$

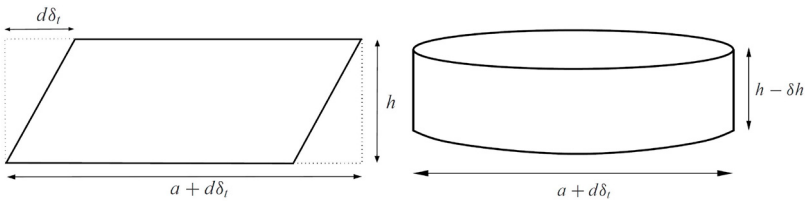


Fig. 5. Geometry change under shear loading.

For mixed-mode loading the upper bound becomes

$$
T_n\dot{\delta}_n + T_t\dot{\delta}_t \leq \sigma_y \int_f^1 \sqrt{\dot{\delta}_n^2\left(1 + \frac{1}{3v^2}\right) + \frac{\dot{\delta}_t^2}{3}}dv \qquad \text{where} \qquad v = \frac{r^2}{l^2}. \tag{8}
$$

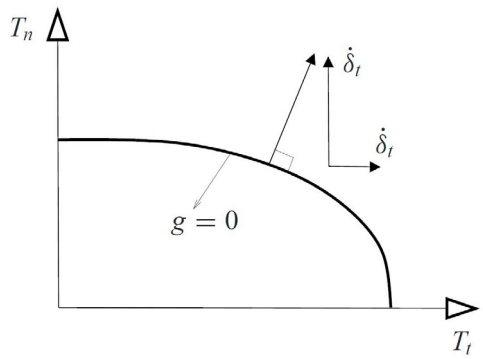


Fig. 6. Yield function representation of normal and tangential traction through Minkowski inequality.

Applying Minkowski inequality gives eventually the following quadratic yield function representation (see also Fig. 6)

$$g = \left[ \frac{T_n^2}{(1-f)^2 + \left(\frac{1}{\sqrt{3}} \ln \frac{1}{f}\right)^2} + \frac{3T_t^2}{(1-f)^2} \right]^{\frac{1}{2}} - \sigma_y = \bar{\sigma} - \sigma_y \tag{9}$$

Both Minkowski inequality and the Jensen's inequality (see Yalcinkaya and Cocks (2015)) give the same functional form of the yield condition under pure mode II loading. The yield function of (9) can be combined with suitable hardening laws for the yield strength $\sigma_y$ to provide an incremental model for variable mixed-mode loading. Noting that,

$$\dot{\delta}_n = \lambda \frac{\partial \bar{\sigma}}{\partial T_n} \qquad \text{and} \qquad \dot{\delta}_t = \lambda \frac{\partial \bar{\sigma}}{\partial T_t} \tag{10}$$

and using

$$\frac{\partial \bar{\sigma}}{\partial T_n} = \frac{T_n}{\left((1-f)^2 + \left(\frac{1}{\sqrt{3}} \ln \frac{1}{f}\right)^2\right)\bar{\sigma}} \qquad \text{and} \qquad \frac{\partial \bar{\sigma}}{\partial T_t} = \frac{3T_t}{(1-f)^2 \bar{\sigma}} \tag{11}$$

The equivalent separation rate is written as follows

$$\lambda = \dot{\delta}_e = \left[ \dot{\delta}_n^2 \left( (1-f)^2 + \left(\frac{1}{\sqrt{3}} \ln \frac{1}{f}\right)^2 \right) + \frac{\dot{\delta}_t^2 (1-f)^2}{3} \right]^{\frac{1}{2}} \tag{12}$$

### 2.3. Work of fracture

The work of fracture could be calculated through the following integral in terms of equivalent traction $\bar{T}$ and equivalent separation $\delta_e$ or through normal and tangential components separately

$$G = \int T_n d\delta_n + T_t d\delta_t = \int \bar{T} d\delta_e \tag{13}$$

Note that $d\delta_n = d\delta_e \frac{\partial \bar{\sigma}}{\partial T_n}$ and $d\delta_t = d\delta_e \frac{\partial \bar{\sigma}}{\partial T_t}$. Therefore

$$G = \int \left( T_n \frac{\partial \bar{\sigma}}{\partial T_n} + T_t \frac{\partial \bar{\sigma}}{\partial T_t} \right) d\delta_e \tag{14}$$

Remember that $\bar{\sigma} = \left[ T_n^2/g_1(f) + T_t^2/g_2(f) \right]^{\frac{1}{2}}$ where

$$g_1(f) = (1-f)^2 + \left( \frac{1}{\sqrt{3}} \ln \frac{1}{f} \right)^2 \quad \text{and} \quad g_2(f) = \frac{(1-f)^2}{3} \tag{15}$$

Then $\frac{\partial \bar{\sigma}}{\partial T_n} = \frac{T_n}{\bar{\sigma} g_1(f)}$ and $\frac{\partial \bar{\sigma}}{\partial T_t} = \frac{T_t}{\bar{\sigma} g_2(f)}$. The integrand in (14) becomes $\left( T_n \frac{\partial \bar{\sigma}}{\partial T_n} + T_t \frac{\partial \bar{\sigma}}{\partial T_t} \right) = \left( \frac{T_n^2}{\bar{\sigma} g_1(f)} + \frac{T_t^2}{\bar{\sigma} g_2(f)} \right)$, and (14) becomes

$$G = \int_{f_0}^{f} \bar{\sigma} d\delta_e = \int_{f_0}^{f} \sigma_y d\delta_e \tag{16}$$

(7) and (12) gives

$$\begin{aligned} d\delta_e &= \left[ d\delta_n^2 g_1(f) + d\delta_t^2 g_2(f) \right]^{\frac{1}{2}} \\ df &= \frac{d\delta_n}{h}(1-f) + 2\sqrt{f}\frac{d\delta_t}{l} \quad \text{and} \quad dh = d\delta_n - \frac{2h}{a} d\delta_t \end{aligned} \tag{17}$$

For proportional loading assume that $d\delta_t / d\delta_n = \alpha$,

$$\begin{aligned} d\delta_e &= d\delta_n \left[ g_1(f) + \alpha^2 g_2(f) \right]^{\frac{1}{2}} \\ df &= d\delta_n \left[ \frac{(1-f)}{h} + 2\sqrt{f}\frac{\alpha}{l} \right] \quad \text{and} \quad dh = d\delta_n \left[ 1 - \frac{2h\alpha}{l\sqrt{f}} \right] \end{aligned} \tag{18}$$

From (18) we get $h$ as a function of $f$

$$\frac{dh}{df} = (1 - \frac{2h\alpha}{l\sqrt{f}})/(\frac{(1-f)}{h} + 2\sqrt{f}\frac{\alpha}{l}) \tag{19}$$

Then substitution of $h$ into $df = d\delta_n((1-f)/h + 2\sqrt{f}(\alpha/l))$ and integration would give $\delta_n$ as a function of $f$. Further integration of (18)-1 would give the work of fracture through (16).

## 3. Concluding remarks

This paper illustrates a physics based derivation of mode–I and mixed–mode traction separation relations in the context of cohesive zone modeling of ductile fracture. The formulation is based on the growth of an array of pores which is the fundamental underlying physical mechanism of ductile fracture, and porous plasticity models used for damage initiation prediction. An upper bound solution is applied for the deformation of the representative volume element and the traction-separation relations are obtained through Minkowski integral inequality for different loading histories and the calculation of the work of fracture is illustrated. The model is going to be used for crack propagation simulations implemented in the interface finite elements, and the initiation is to be governed by a consistent porous plasticity model implemented in bulk finite elements. In this way the crack initiation and propagation steps could be simulated through physically consistent models.

## References


Barbee, T.W., Seaman, L., Crewdson, R., Curran, D., 1972. Dynamic fracture criteria for ductile and brittle metals. J. Mater. 7, 393–401.

Barenblatt, G.I., 1962. The mathematical theory of equilibrium cracks in brittle fracture. Adv. Appl. Mech. 7, 55–129.

Beachem, C.D., Yoder, G.R., 1973. Elastic-plastic fracture by homogeneous microvoid coalescence tearing along alternating shear planes. Metall. Trans. 4, 1145–1153.

Brocks, W., Cornec, A., Scheidern, I., 2003. Computational aspects of nonlinear fracture mechanics. Comprehensive Structural Integrity - Numerical and Computational Methods 3, 127–209.

Cocks, A.C.F., 1989. Inelastic deformation of porous materials. J. Mech. Phys. Solids 37, 693–715.

Cocks, A.C.F., Ashby, M.F., 1980. Intergranular fracture during power-law creep under multiaxial stresses. Metal Science 14, 395–402.

Cortes, R., 1992. Dynamic growth of microvoids under combined hydrostatic and deviatoric stresses. Int. J. Solids Struct. 29, 1637–1645.

Fleck, N.A., Hutchinson, J.W., 1986. Void growth in shear. Proc. R. Soc. A 407, 435–458.

Gologanu, M., Leblond, J.B., Devaux, J., 1993. Approximate models for ductile metals containing non-spherical voidscase of axisymmetric prolate ellipsoidal cavities. J. Mech. Phys. Solids 41, 1723–1754.

Gologanu, M., Leblond, J.B., Devaux, J., 1994. Approximate models for ductile metals containing nonspherical voidscase of axisymmetric oblate ellipsoidal cavities. J. Eng. Mater. Technol. (Trans. ASME) 116, 290–297.

Gurson, A., 1977. Continuum theory of ductile rupture by void nucleation and growth: Part i - yield criteria and flow rules for porous ductile media. Journal of Engineering Materials and Technology 99, 2–15.

Hardy, G., Littlewood, J.E., Polya, G., 1996. Inequalities. Cambridge University Press .

Marin, E.B., McDowell, D.L., 1996. Associative versus non-associative porous viscoplasticity based on internal state variable concepts. Int. J. Plasticity 12, 629–669.

McClintock, F.A., 1968. A criterion for ductile fracture by growth of holes. J. Appl. Mech. 35, 363–371.

Rousselier, G., 1987. Ductile fracture models and their potential in local approach of fracture. Nucl. Eng. Des. 105, 97–111.

Thomason, P.F., 1990. Ductile fracture of metals. Pergamon .

Tvergaard, V., 1990. Material failure by void growth to coalescence. Adv. Appl. Mech. 27, 83–151.

Tvergaard, V., Hutchinson, J.W., 1992. The relation between crack growth resistance and fracture process parameters in elastic-plastic solids. J. Mech. Phys. Solids 40, 1377–1397.

Tvergaard, V., Needleman, A., 1984. Analysis of the cup-cone fracture in a round tensile bar. Acta Metall. Mater. 32, 157–169.

Yalcinkaya, T., Cocks, A., 2015. Physics based formulation of a cohesive zone model for ductile fracture. Key Eng. Mat. 651–653, 993–999.